



# $\mu$ -Halo bridged binuclear ruthenium(III) complexes featuring pyridazine ligands: Synthesis, structure, spectral and electrochemical properties

Devaraj Pandiarajan, Rengan Ramesh\*

School of Chemistry, Bharathidasan University, Tiruchirappalli 620 024, India

## ARTICLE INFO

### Article history:

Received 16 November 2011

Accepted 19 December 2011

Available online 11 January 2012

### Keywords:

Binuclear ruthenium(III)

Pyridazine ligand

Crystal structure

Redox behavior

## ABSTRACT

The reaction of  $[\text{RuX}_3(\text{AsPh}_3)_3]$  and *N,N*-disubstituted pyridazine-3,6-diamine in benzene under reflux afford novel binuclear, halo-bridged, ruthenium(III) complexes with the general formula  $[\text{Ru}_2(\text{AsPh}_3)_2(\mu\text{-X})_2\text{X}_4(\text{L})]$  ( $\text{X} = \text{Cl}$  or  $\text{Br}$ ;  $\text{L} = \text{N,N}$ -disubstituted pyridazine-3,6-diamine). All the complexes have been characterized by elemental analysis, spectral (UV–Vis, EPR) and electrochemical methods (CV, DPV). The electronic spectra of the complexes indicate the presence of *d–d* and intense LMCT transitions in the visible region. The molecular structure of one of the complexes (**2**) has been determined by X-ray crystallography, which indicates the bridging coordination of the pyridazine in these binuclear complexes. In complex (**2**) each metal has a distorted octahedral  $\text{NCl}_4\text{As}$  coordination sphere constituted by the two exogenous bridging chlorides. The complexes are paramagnetic (low spin,  $d^5$ ) in nature and all the complexes at 77 K show rhombic distortion around the ruthenium ion with three different 'g' values ( $g_x \neq g_y \neq g_z$ ). All the complexes exhibit two quasi-reversible one electron reductive responses ( $\text{Ru}^{\text{III}}\text{-Ru}^{\text{III}}/\text{Ru}^{\text{II}}\text{-Ru}^{\text{III}}$ ;  $\text{Ru}^{\text{II}}\text{-Ru}^{\text{III}}/\text{Ru}^{\text{II}}\text{-Ru}^{\text{II}}$ ) within the  $E_{1/2}$  range of  $-0.68$  to  $-0.78$  V and  $-1.25$  to  $-1.33$  V, respectively, versus SCE.

© 2012 Elsevier Ltd. All rights reserved.

## 1. Introduction

Renewed interest in pyridazine chemistry arises from the potential that they have shown in the formation of polynuclear coordination assemblies with diverse topologies. Generally transition metal complexes of pyridazine containing ligands have produced a large number of metal complexes with a wide range of interesting magnetic, electrochemical and structural properties [1–4]. As  $\pi$ -delocalized ligands with a low  $\pi^*$  level and strong  $\pi$ -accepting character, pyridazine ligands have been widely utilized in the construction of polynuclear complexes. Pyridazine units have been incorporated into numerous systems including acyclic ligands, [5,6] coordination polymers [7], cryptands [8–10] and also macrocycles [11–14]. The diazine, *N–N*, fragment found in the pyridazine and phthalazine entities, are the common focus of these binucleating ligands. Ligands of the type OXP, DCPZ and PTP, PPD and DPPN (Fig. 1) generate six-membered chelate rings. Although there have been several studies involving binucleating ligands which contain the 1,2-diazine link [15–17], reports on complexes in which pyridazine itself acts as a bridging ligand remain relatively rare. The electron-deficient aromatic system, containing two potential N-donor atoms, leads to a decrease the electron-donor abilities in comparison to pyridines, which is reflected by significantly lower

$pK_a$  values (2.24 for the parent pyridazine versus 5.25 for pyridine) [18].

The two vicinal nitrogen donor atoms in the pyridazine and phthalazine heterocycles allow, in principle, the coordination of two metal centers in close proximity and provide an intramolecular pathway for spin exchange interactions, which are exclusively antiferromagnetic in nature [19–22]. Furthermore, the orientation of the nitrogen lone pairs allows bridging coordination on suitable metal fragments. Often they are also bridged by other groups such as hydroxide [23,24], halogen [25], sulfate [26], nitrate [15], iodate [27] or azide [28]. However, in non-macrocyclic ligands, two additional donor sites attached to the aromatic ring on both sides of the nitrogen atoms (3,6-positions) or secondary bridging ligands seem to be a prerequisite to accommodate two or more metal atoms in elaborate structures [1,14,29,30]. Thus, pyridazines without adjacent coordination sites act mostly as bidentate ligands [31]. These structural, magnetic and electrochemical studies followed on from earlier work by Blake and co-workers, who were the first to look at the magnetic exchange between metal ions bridged by pyridazine- and phthalazine-containing ligands [32–35].

The earliest studies relevant to our work are those by Thompson and co-workers, who have been the key players in the development of magneto structural data on pyridazine and phthalazine-bridged acyclic dicopper(II) complexes [25,36,37]. Brooker et al. developed a methodology concerning the synthesis and structural characterization of transition metal complexes of Schiff-base macrocycles

\* Corresponding author. Fax: +91 431 2407045/2407020.

E-mail address: [ramesh\\_bdu@yahoo.com](mailto:ramesh_bdu@yahoo.com) (R. Ramesh).

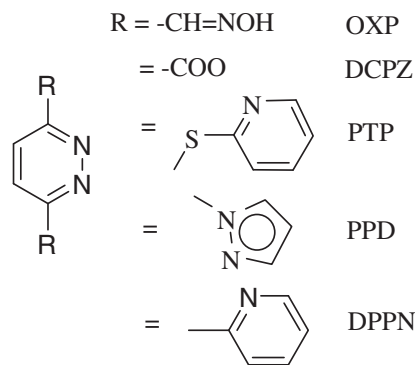
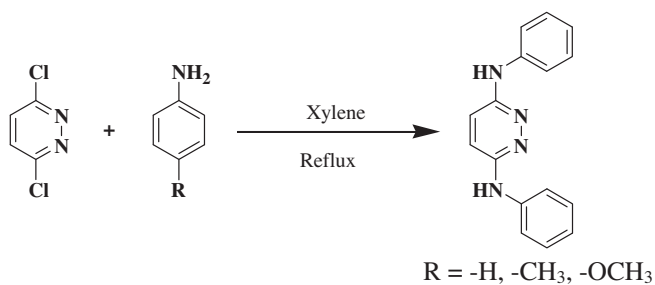
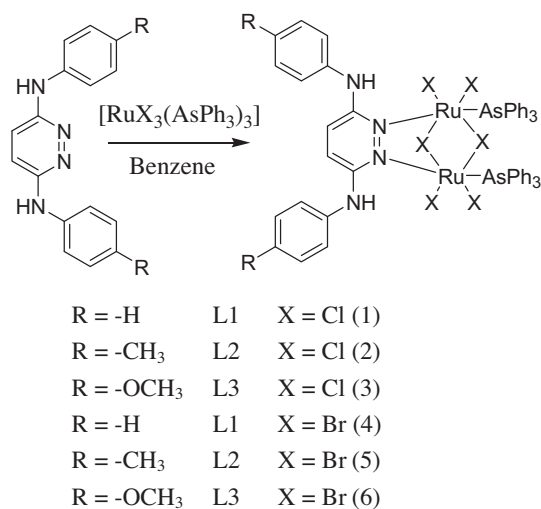


Fig. 1. Dinucleating diazine ligands.



Scheme 1. Synthesis of the ligands.



Scheme 2. Formation of the binuclear ruthenium pyridazine complexes.

containing pyridazine head units [13,5,38]. Escuer et al. reported the synthesis, structure and magnetic behavior of two new nickel(II) and cobalt(II) binuclear complexes with 1,4-dicarboxylatopyridazine and their MO calculations of the super exchange pathway through the pyridazine bridge [39].

Further, doubly cyclometallated palladium(II) acetate complexes containing 3,6-diphenylpyridazine have been described [40]. Supramolecular networks assembled from zinc and manganese binuclear complexes with pyridazine-3,6-dicarboxylate have been reported [41]. A novel class of luminescent tricarbonyl rhenium(I) complexes containing bridging 1,2-diazine ligands has also been described [42]. Mashima and co-workers synthesized the binuclear palladium complexes of 3,6-bis(imino(2,6-diisopropylphenyl))pyridazine

ligands containing a  $\mu$ -chloro bridge between the two metal atoms [43]. Further, Zanetti and co-workers reported Schiff base ligands containing pyridazine ligands with first-row transition metals [44]. Sun and co-workers described the synthesis and characterization of 3,6-dipyridyl substituted pyridazine biruthenium complexes and the catalytic activity of these complexes towards oxidation of water to molecular oxygen evolution [45]. These observations clearly indicate that our pyridazine-containing ligands are, as one might expect on the basis of their  $\pi$ -acceptor properties, good at stabilizing low oxidation states of transition metal ions. Hence, we turned our attention towards pyridazine ligands modified with two arms, based on their earlier reports and their catenation property.

We have long been involved in the synthesis and catalytic applications of new ruthenium(III) complexes with different ligand systems, such as arylazophenols and Schiff bases [46–48]. The present work stems from our interest to design novel  $\mu$ -halo bridged binuclear pyridazine ruthenium complexes of the type  $[\text{Ru}_2(\text{AsPh}_3)_2(\mu\text{-X})_2\text{X}_4(\text{L})]$ , involving triphenylarsine as an ancillary functionality. The molecular structure of complex **2** has been established by single-crystal X-ray analysis, in combination with electronic and EPR spectra. The relative stabilities of the oxidation and reduction states are examined electrochemically.

## 2. Experimental

### 2.1. Materials

All reagents and solvents were of high purity grade and were purchased from commercial sources and used as received unless noted otherwise. Commercial  $\text{RuCl}_3 \cdot 3\text{H}_2\text{O}$  was purchased from Loba-Chemie Pvt. Ltd. The solvents were purified and dried according to standard procedures. 3,6-Dichloropyridazine and the aniline derivatives were obtained from Aldrich. The supporting electrolyte, tetrabutyl ammonium perchlorate ( $n\text{-Bu}_4\text{NClO}_4$ ), was dried in vacuum prior to use. The starting precursor complexes,  $[\text{RuCl}_3(\text{AsPh}_3)_3]$  [49] and  $[\text{RuBr}_3(\text{AsPh}_3)_3]$  [50], were prepared according to the reported procedure.

### 2.2. Physical measurements

Microanalytical (C, H, N) data were obtained with a Perkin-Elmer model 240C elemental analyzer. The solution electrical conductivity was obtained using a Systronic 305 conductivity bridge.  $^1\text{H}$  NMR spectra were recorded with a Bruker 400 MHz spectrometer. All  $^1\text{H}$  and  $^{13}\text{C}$  NMR spectra were taken in pure deuterated DMSO solvent. Chemical shifts ( $\delta$ ) are given in ppm and refer to TMS as an internal standard. The EPR measurements were carried out with an X-band (9.5 GHz) JEOL FA200 spectrometer. Electrochemical measurements were performed in a conventional two-compartment cell with a polished glassy carbon working electrode, Pt wire as a counter electrode and a saturate calomel electrode (SCE) as the reference electrode. All the electrochemical measurements were carried out with CHI model 650B (Austin, TX) electrochemical workstation. The supporting electrolyte was 0.1 M  $[(n\text{-C}_4\text{H}_9)_4\text{N}](\text{ClO}_4)$  (TBAP), and the solute concentration was ca.  $10^{-3}$  M. The half-wave potential  $E^0$  298 was set equal to  $0.5(E_{\text{pa}} + E_{\text{pc}})$ , where  $E_{\text{pa}}$  and  $E_{\text{pc}}$  are the anodic and cathodic cyclic voltammetric peak potentials, respectively.

### 2.3. Synthesis of the ligands

#### 2.3.1. *N,N'*-Diphenyl-pyridazine-3,6-diamine (L1)

A mixture of 3,6-dichloropyridazine (0.5 g, 3.356 mmol) and aniline (0.625 g, 6.71 mmol) in 40 cm<sup>3</sup> of xylene was heated in

**Table 1**  
Analytical data for the binuclear ruthenium(III) pyridazine complexes.

Complexes	Empirical formula	Color	M.p.	Calculated (found) (%)		
				C	H	N
<b>1</b>	C <sub>52</sub> H <sub>44</sub> As <sub>2</sub> Cl <sub>6</sub> N <sub>4</sub> Ru <sub>2</sub>	Green	195–198	48.43(48.39)	3.44(3.40)	4.34(4.30)
<b>2</b>	C <sub>54</sub> H <sub>48</sub> As <sub>2</sub> Cl <sub>6</sub> N <sub>4</sub> Ru <sub>2</sub>	Green	212–216	49.22(49.20)	3.67(3.71)	4.25(4.21)
<b>3</b>	C <sub>54</sub> H <sub>48</sub> As <sub>2</sub> Cl <sub>6</sub> N <sub>4</sub> O <sub>2</sub> Ru <sub>2</sub>	Green	210–216	48.05(48.10)	3.58(3.62)	4.15(4.19)
<b>4</b>	C <sub>52</sub> H <sub>44</sub> As <sub>2</sub> Br <sub>6</sub> N <sub>4</sub> Ru <sub>2</sub>	Green	218–223	40.13(40.18)	2.85(2.80)	3.60(3.63)
<b>5</b>	C <sub>54</sub> H <sub>48</sub> As <sub>2</sub> Br <sub>6</sub> N <sub>4</sub> Ru <sub>2</sub>	Green	198–204	40.94(40.88)	3.05(3.09)	3.54(3.57)
<b>6</b>	C <sub>54</sub> H <sub>48</sub> As <sub>2</sub> Br <sub>6</sub> N <sub>4</sub> O <sub>2</sub> Ru <sub>2</sub>	Green	221–225	40.13(40.11)	2.99(2.95)	3.47(3.51)

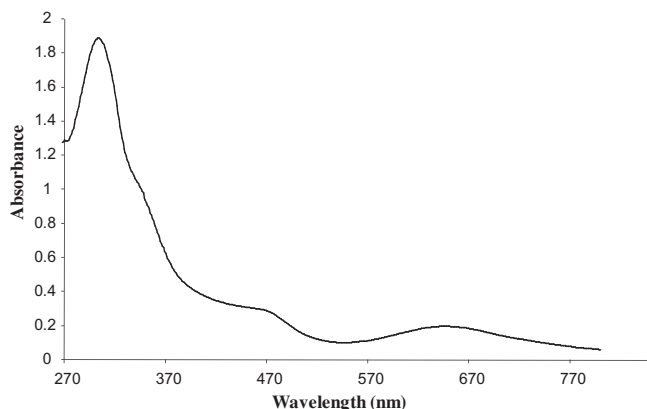


**Fig. 2.** Electronic absorption spectrum of [Ru<sub>2</sub>(AsPh<sub>3</sub>)<sub>2</sub>(μ-Cl)<sub>2</sub>Cl<sub>4</sub>(L<sub>2</sub>)] (**2**) in CH<sub>3</sub>CN.

**Table 2**  
Electronic spectra of the binuclear ruthenium(III) pyridazine complexes

Complexes	λ <sub>max</sub> (nm)	ε (dm <sup>3</sup> /mol/cm)	
<b>1</b>	648(4587) <sup>a</sup>	471(6133) <sup>b</sup>	287(9642) <sup>c</sup>
<b>2</b>	631(1968) <sup>a</sup>	462(2968) <sup>b</sup>	302(18,825) <sup>f</sup>
<b>3</b>	635(1819) <sup>a</sup>	458(2292) <sup>b</sup>	287(6584) <sup>c</sup>
<b>4</b>	651(2673) <sup>a</sup>	452(4873) <sup>b</sup>	280(6558) <sup>c</sup>
<b>5</b>	647(1974) <sup>a</sup>	465(2968) <sup>b</sup>	288(6283) <sup>c</sup>
<b>6</b>	661(2662) <sup>a</sup>	462(4683) <sup>b</sup>	285(6587) <sup>c</sup>

<sup>a</sup> *d-d* Transition.

<sup>b</sup> LMCT.

<sup>c</sup> Ligand centered transition (LCT).

an oil bath at 150 °C with continuous stirring for 6 h. The oil bath was removed and after the mixture was cooled briefly, 30 cm<sup>3</sup> of water was added cautiously with stirring, followed by the addition of 0.5 g solid sodium hydroxide. To the mixture, cooled to room temperature (RT), 50 cm<sup>3</sup> dichloromethane was added and the suspension was stirred until the yellow lumps that had formed were loosened to a yellow powder. The powder was filtered, washed with water and diethyl ether, dried in air and then recrystallized from hot acetone. Yield: 0.859 g, 97%. M.p. 241 °C. <sup>1</sup>H NMR (400 MHz, DMSO-*d*<sub>6</sub>, Me<sub>4</sub>Si) δ: 7.12 (2H, t, Ar-H), 7.39 (4H, t, Ar-H), 7.53 (4H, d, Ar-H), 7.67 (2H, s, py-H), 10.46 (2H, br s, NH). <sup>13</sup>C NMR (100 MHz, DMSO-*d*<sub>6</sub>, Me<sub>4</sub>Si) δ: 120.83, 124.18, 126.72, 129.25, 137.72, 149.12 (aromatic carbons).

### 2.3.2. *N,N'*-Di-*p*-tolyl-pyridazine-3,6-diamine (L<sub>2</sub>)

Yield: 0.916 g, 92%. M.p. 228 °C. <sup>1</sup>H NMR (400 MHz, DMSO-*d*<sub>6</sub>, Me<sub>4</sub>Si) δ: 2.23 (6H, s, CH<sub>3</sub>), 7.08 (4H, d, Ar-H), 7.15 (2H, s, py-H), 7.57 (4H, d, Ar-H), 9.09 (2H, br s, NH). <sup>13</sup>C NMR (100 MHz, DMSO-*d*<sub>6</sub>, Me<sub>4</sub>Si) δ: 20.34 (CH<sub>3</sub>), 118.13, 118.9, 120, 121, 129, 129.3, 138.5, 151.6 (aromatic carbons).

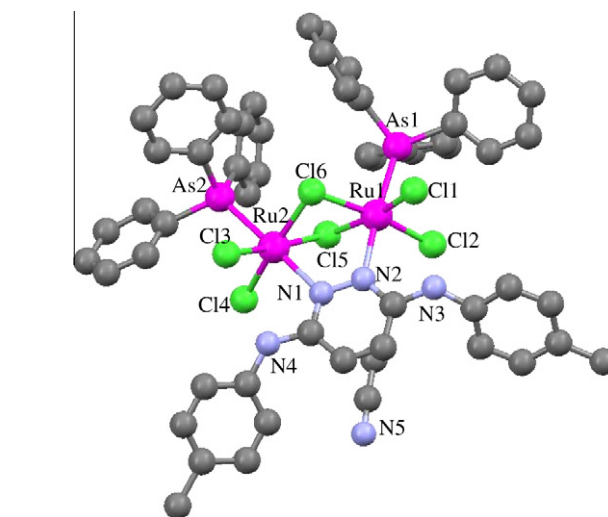


**Fig. 3.** ORTEP diagram of [Ru<sub>2</sub>(AsPh<sub>3</sub>)<sub>2</sub>(μ-Cl)<sub>2</sub>Cl<sub>4</sub>(L<sub>2</sub>)] showing 50% probability thermal ellipsoids.

### 2.3.3. *N,N'*-Bis-(4-methoxy-phenyl)-pyridazine-3,6-diamine (L<sub>3</sub>)

Yield: 0.982 g, 91%. M.p. 232 °C. <sup>1</sup>H NMR (400 MHz, DMSO-*d*<sub>6</sub>, Me<sub>4</sub>Si) δ: 3.77 (6H, s, OCH<sub>3</sub>), 6.91 (4H, d, Ar-H), 7.04 (2H, s, py-H), 7.67 (4H, d, Ar-H), 8.70 (2H, br s, NH). <sup>13</sup>C NMR (100 MHz, DMSO-*d*<sub>6</sub>, Me<sub>4</sub>Si) δ: 55.12 (OCH<sub>3</sub>), 113.85, 119.05, 119.66, 135.21, 152.07, 153.15 (aromatic carbons).

## 2.4. Synthesis of the complexes

### 2.4.1. General procedure

A degassed benzene solution of [RuCl<sub>3</sub>(AsPh<sub>3</sub>)<sub>3</sub>] or [RuBr<sub>3</sub>(PPh<sub>3</sub>)] (2 mmol) was taken in a clean 100 ml round bottom flask. The *N,N*-disubstituted pyridazine-3,6-diamine ligands (1 mmol) were added to the above solution. The mixture was heated at reflux for 8 h. The initial brown red color of the solution gradually changed to green. The solvent was then evaporated under high vacuum at low temperature, which followed by petroleum ether (60–80 °C) workup gave a green colored solid. The solid mass thus obtained was purified using a silica column (60–120 mesh) chromatography. On elution with chloroform and methanol solvents, the green band of the expected product was isolated. Single crystals suitable for X-ray diffraction analysis were grown from mixture of chloroform–acetonitrile solution at room temperature.

### 2.5. X-ray crystallography

Single crystals of [Ru<sub>2</sub>(AsPh<sub>3</sub>)<sub>2</sub>(μ-Cl)<sub>2</sub>Cl<sub>4</sub>(L<sub>2</sub>)]·CH<sub>3</sub>CN (**2**) were grown by slow evaporation of a chloroform–acetonitrile solution at room temperature. A crystal of dimensions 0.30 × 0.26 × 0.22 mm was selected and the data were collected. The crystal was mounted on the top of a glass fiber, and transferred to a Stoe IPDS

**Table 3**Crystal data and structure refinement for the binuclear ruthenium(III) pyridazine complex (**2**).

Empirical formula	C <sub>56</sub> H <sub>49</sub> As <sub>2</sub> Cl <sub>6</sub> N <sub>5</sub> Ru <sub>2</sub>
Formula weight	1356.68
Temperature (K)	296(2)
Wavelength (Å)	0.71073
Crystal system, space group	triclinic, P $\bar{1}$
<i>Unit cell dimensions</i>	
<i>a</i> (Å)	10.7679(6)
<i>b</i> (Å)	16.6809(11)
<i>c</i> (Å)	17.7289(10)
$\alpha$ (°)	90.624(4)
$\beta$ (°)	102.277(4)
$\gamma$ (°)	108.369(4)
Volume (Å <sup>3</sup> )	2942.6(3)
<i>Z</i> , Calc. density (mg/m <sup>3</sup> )	2, 1.531
Absorption coefficient (mm <sup>-1</sup> )	1.941
<i>F</i> (000)	1352
Crystal size (mm)	0.30 × 0.26 × 0.22
Theta range for data collection	1.18–23.67°
Limiting indices	–12 ≤ <i>h</i> ≤ 12, –18 ≤ <i>k</i> ≤ 18, –19 ≤ <i>l</i> ≤ 19
Reflections collected/unique	44 122/8789 ( <i>R</i> <sub>int</sub> = 0.1596)
Completeness to 2 $\theta$	23.67, 98.9%
Absorption correction	semi-empirical from equivalents
Maximum and minimum transmission	0.6747 and 0.5936
Refinement method	full-matrix least-squares on <i>F</i> <sup>2</sup>
Data/restraints/parameters	8789/0/643
Goodness-of-fit (GOF) on <i>F</i> <sup>2</sup>	1.038
Final <i>R</i> indices [ <i>I</i> > 2 $\sigma$ ( <i>I</i> )]	<i>R</i> <sub>1</sub> = 0.0773, <i>wR</i> <sub>2</sub> = 0.1845
<i>R</i> indices (all data)	<i>R</i> <sub>1</sub> = 0.1367, <i>wR</i> <sub>2</sub> = 0.2064
Largest diff. peak and hole (e Å <sup>-3</sup> )	1.717 and –1.051

diffractometer using monochromated Mo K $\alpha$  radiation (*kl* = 0.71073). Corrections were made for Lorentz and polarization effects as well as for absorption (numerical). The structures were solved and refined by full-matrix least-squares techniques on *F*<sup>2</sup> using the SHELX 97 program [51,52]. The absorption corrections were done by the multi scan technique. All data were corrected for Lorentz and polarization effects, and the non-hydrogen atoms were refined anisotropically. Hydrogen atoms were included in the refinement process as per the riding model.

### 3. Results and discussion

#### 3.1. Synthesis of the *N,N*-disubstituted pyridazine-3,6-diamine ligands

Ligands of this sort have been synthesized by the very effective nucleophilic displacement of chlorine from 3,6-dichloropyridazine by *p*-substituted aniline in refluxing xylene, which followed by subsequent workup gave the *N,N*-disubstituted pyridazine-3,6-diamine as a free flowing solid in high isolated yields (Scheme 1) [53]. The *p*-methyl substituted ligand is obtained as a yellow solid, the *p*-methoxy derivative as a green solid and the aniline derivative as an orange solid. All the ligands are characterized by <sup>1</sup>H and <sup>13</sup>C {<sup>1</sup>H} NMR in DMSO-*d*<sub>6</sub>.

#### 3.2. Synthesis of the complexes

All the complexes are synthesized by refluxing a benzene solution of 1 mole of the ligand with 2 moles of [Ru(AsPh<sub>3</sub>)<sub>3</sub>X<sub>3</sub>] (*X* = Cl, Br) under a nitrogen atmosphere for 8 h (Scheme 2). Coordination was immediate, as a change of color from reddish brown to a green color was apparent. The solvent was then removed under high vacuum at low temperature followed by dichloromethane and petroleum ether workup to give a green colored solid. The solid residue thus obtained was purified using a silica gel column by

**Table 4**Selected bond angles (°) and bond lengths (Å) for complex **2**.

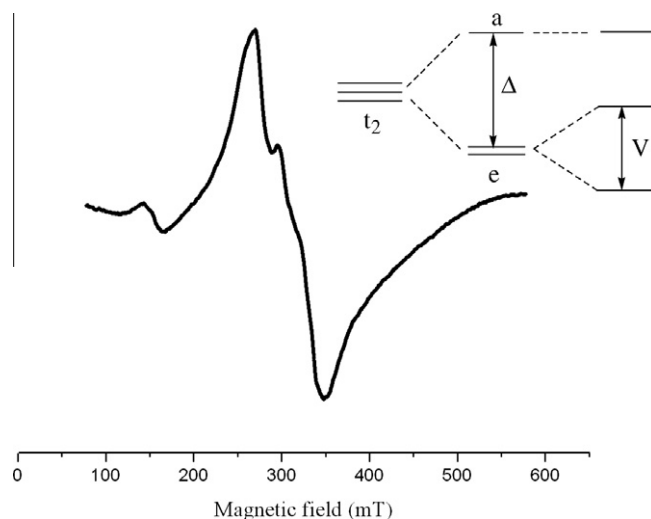
<i>Bond length</i>			
As(1)–Ru(1)	2.4423(12)	As(2)–Ru(2)	2.4453(13)
Cl(6)–Ru(1)	2.392(3)	Cl(6)–Ru(2)	2.381(3)
Cl(5)–Ru(1)	2.383(3)	Cl(5)–Ru(2)	2.375(3)
N(2)–Ru(1)	2.185(7)	N(1)–Ru(2)	2.212(7)
Cl(2)–Ru(1)	2.307(3)	Cl(3)–Ru(2)	2.346(3)
Cl(1)–Ru(1)	2.327(3)	Cl(4)–Ru(2)	2.316(3)
N(1)–N(2)	1.368(10)		
<i>Bond angles</i>			
N(2)–Ru(1)–As(1)	175.0(2)	N(1)–Ru(2)–As(2)	178.5(2)
Cl(2)–Ru(1)–Cl(6)	171.53(10)	Cl(4)–Ru(2)–Cl(6)	171.36(11)
Cl(1)–Ru(1)–Cl(5)	169.83(10)	Cl(3)–Ru(2)–Cl(5)	172.79(11)
Cl(6)–Ru(1)–As(1)	98.35(7)	Cl(6)–Ru(2)–As(2)	93.35(7)
Cl(5)–Ru(1)–As(1)	95.01(7)	Cl(5)–Ru(2)–As(2)	96.15(7)
Cl(1)–Ru(1)–As(1)	85.38(7)	Cl(3)–Ru(2)–As(2)	85.38(9)
Cl(2)–Ru(1)–As(1)	85.55(8)	Cl(4)–Ru(2)–As(2)	86.85(9)
N(2)–Ru(1)–Cl(1)	94.3(2)	N(1)–Ru(2)–Cl(3)	93.2(2)
N(2)–Ru(1)–Cl(2)	89.6(2)	N(1)–Ru(2)–Cl(4)	93.0(2)
N(2)–Ru(1)–Cl(5)	86.2(2)	N(1)–Ru(2)–Cl(5)	85.3(2)
N(2)–Ru(1)–Cl(6)	86.7(2)	N(1)–Ru(2)–Cl(6)	87.0(2)
Cl(1)–Ru(1)–Cl(6)	87.02(10)	Cl(3)–Ru(2)–Cl(6)	89.61(11)
Cl(2)–Ru(1)–Cl(5)	89.32(10)	Cl(4)–Ru(2)–Cl(5)	88.12(11)
Cl(5)–Ru(1)–Cl(6)	82.87(9)	Cl(5)–Ru(2)–Cl(6)	83.27(9)
Cl(2)–Ru(1)–Cl(1)	100.84(10)	Cl(4)–Ru(2)–Cl(3)	99.00(12)
N(1)–N(2)–Ru(1)	116.7(5)	N(2)–N(1)–Ru(2)	116.0(5)
Ru(2)–Cl(5)–Ru(1)	88.52(8)	Ru(2)–Cl(6)–Ru(1)	88.16(9)

**Table 5**

EPR data of the binuclear ruthenium(III) pyridazine complexes.

Complexes	<i>g</i> <sub>x</sub>	<i>g</i> <sub>y</sub>	<i>g</i> <sub>z</sub>	( <i>g</i> <sup>*</sup> )
<b>1</b>	2.54	2.07	1.85	2.17
<b>2</b>	2.49	2.18	1.94	2.22
<b>3</b>	2.49	2.22	1.96	2.24
<b>4</b>	2.46	2.23	1.93	2.21
<b>5</b>	2.45	2.06	1.89	2.15
<b>6</b>	2.55	2.04	1.85	2.16

$$(g^*) = [1/3 g_x^2 + 1/3 g_y^2 + 1/3 g_z^2]^{1/2}$$

**Fig. 4.** EPR spectrum of [Ru<sub>2</sub>(AsPh<sub>3</sub>)<sub>2</sub>(μ-Cl)<sub>2</sub>Cl<sub>4</sub>(L1)] at 77 K.

elution with chloroform and methanol, giving a green colored band corresponding to the desired product. All the synthesized complexes were found to be air stable in both the solid and the liquid states at room temperature and were non-hygroscopic in nature. The synthesized binuclear ruthenium(III) pyridazine complexes

**Table 6**  
Redox potentials for the binuclear ruthenium(III) pyridazine complexes.<sup>a</sup>

Complexes	Ru <sup>(III)</sup> –Ru <sup>(III)</sup> /Ru <sup>(II)</sup> –Ru <sup>(III)</sup>				Ru <sup>(II)</sup> –Ru <sup>(III)</sup> /Ru <sup>(II)</sup> –Ru <sup>(II)</sup>			
	<i>E</i> <sub>pc</sub> (V)	<i>E</i> <sub>pa</sub> (V)	<i>E</i> <sub>1/2</sub> (V) <sup>b</sup>	$\Delta E$ (mV) <sup>c</sup>	<i>E</i> <sub>pc</sub> (V)	<i>E</i> <sub>pa</sub> (V)	<i>E</i> <sub>1/2</sub> (V) <sup>b</sup>	$\Delta E$ (mV) <sup>c</sup>
<b>1</b>	–0.79	–0.68	–0.74	110	–1.44	–1.19	–1.32	249
<b>2</b>	–0.78	–0.64	–0.71	137	–1.41	–1.19	–1.30	219
<b>3</b>	–0.79	–0.67	–0.73	117	–1.45	–1.20	–1.33	250
<b>4</b>	–0.81	–0.66	–0.74	150	–1.48	–1.16	–1.32	200
<b>5</b>	–0.73	–0.63	–0.68	105	–1.37	–1.12	–1.25	251
<b>6</b>	–0.75	–0.62	–0.68	132	–1.42	–1.15	–1.29	272

<sup>a</sup> Potential data in volts vs. *F*<sub>c</sub>/*F*<sub>c</sub> are from single scan cyclic voltammograms recorded at 25 °C in a 0.1 M acetonitrile solution of NBu<sub>4</sub>ClO<sub>4</sub> (0.1 M); scan rate: 50 mV s<sup>–1</sup>. Detailed experimental conditions are given in Section 2.

<sup>b</sup>  $E_{1/2} = 1/2(E_{pa} + E_{pc})$ .

<sup>c</sup>  $E = E_{pa} - E_{pc}$  denotes the potential difference between the anodic and cathodic potentials, respectively.

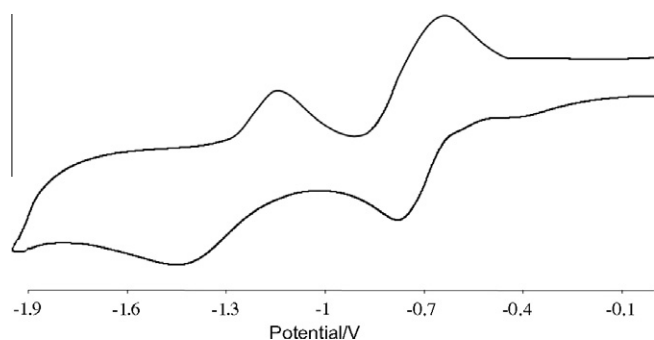


**Fig. 5.** Cyclic voltammograms of **5** in CH<sub>3</sub>CN/0.1 M Bu<sub>4</sub>NClO<sub>4</sub> versus SCE at 298 K (scan rate 50 mV s<sup>–1</sup>).

are soluble in acetonitrile, DMF and DMSO producing intense green colored solutions and they are insoluble in alkanes.

X-ray quality crystals of the complex were grown by slow evaporation of chloroform and acetonitrile solutions to give a pyridazine-coordinated diruthenium bridging complex. Elemental analyses data assigned to the molecular formula [Ru<sub>2</sub>(AsPh<sub>3</sub>)<sub>2</sub>(μ-X)<sub>2</sub>X<sub>4</sub>(L)] are presented in Table 1.

### 3.3. Electronic spectra

Absorption spectral studies are the easiest means of characterizing ruthenium (III) complexes. Electronic spectra of all the complexes have been recorded in dry acetonitrile solution in the range 200–800 nm. The ground state of ruthenium(III) in an octahedral environment is <sup>2</sup>T<sub>2g</sub>, arising from the t<sup>5</sup><sub>2g</sub> configuration, and the first excited doublet levels in the order of increasing energy are <sup>2</sup>A<sub>2g</sub> and <sup>2</sup>T<sub>1g</sub>, arising from the t<sup>4</sup><sub>2g</sub>e<sup>1</sup><sub>g</sub> configuration. Hence, two bands corresponding to <sup>2</sup>T<sub>2g</sub> → <sup>2</sup>A<sub>2g</sub> and <sup>2</sup>T<sub>2g</sub> → <sup>2</sup>T<sub>1g</sub> are possible. A selected spectrum of complex **2** is shown in Fig. 2 and the spectral data of all the complexes are given in Table 2. All the complexes display three intense absorptions in the region 725–255 nm. The absorption spectra of the binuclear ruthenium complexes exhibit very intense bands below 400 nm assigned to ligand-centered (LC) π → π\* transitions, and moderately intense bands located in the visible region from 486 to 435 nm that are ascribed to ligand to metal charge-transfer (LMCT) transitions taking place from the filled ligand (HOMO) orbital to the singly-occupied ruthenium t<sub>2</sub> orbital (HOMO). A broad band appearing between 553 and 724 nm is a characteristic band for a d–d transition. The pattern of the electronic spectra of all the complexes indicates the presence of an octahedral environment around ruthenium(III) that is similar to that of other ruthenium(III) octahedral complexes [54].

### 3.4. Description of the structure

The molecular structure of one of the complexes (**2**) has been determined by single crystal X-ray analysis, and the ORTEP view is shown in Fig. 3. A summary of single crystal X-ray structure refinement and selected bond lengths and bond angles are given in Tables 3 and 4, respectively. The complex [Ru<sub>2</sub>(AsPh<sub>3</sub>)<sub>2</sub>(μ-Cl)<sub>2</sub>Cl<sub>4</sub>(L<sub>2</sub>)] (**2**) was crystallized with CH<sub>3</sub>CN as the solvent for crystallization. The structure consists of a binuclear ruthenium complex bridged by chlorides and both ruthenium atoms are in a distorted octahedral coordination environment. Each ruthenium contains two terminal chlorides, two bridged chloro ligands, one triphenylarsine and one of the nitrogen atoms from the pyridazine ligand. As expected, the Ru<sub>2</sub>(μ-Cl)<sub>2</sub> unit is not planar due to the presence of the pyridazine ring. The angle between the planes containing Cl(5)–Ru(1)–Cl(6) is 82.87(9)° and Cl(5)–Ru(2)–Cl(6) is 83.27(9)°. The terminal chlorine atoms are trans to the bridging chlorine atoms and the AsPh<sub>3</sub> molecules coordinate through As atoms at the trans sites of the pyridazine nitrogens. The Ru–N(pyridazine) distances, N(2)–Ru(1) 2.185(7) and N(1)–Ru(2) 2.212(7) Å (Table 2) are similar to those reported for ruthenium complexes containing the same coordinating atoms [55]. A major perturbation of the structure is observed due to the bridging coordination nature of the pyridazine molecule. Since the lone pairs of two nitrogen atoms effectively interact with each metal atom, the two ruthenium-centered octahedra may bend toward the bridging ligand. The Ru(III)–As distances, As(1)–Ru(1) 2.4423(12) and As(2)–Ru(2) 2.4453(13) Å, are comparatively equal. The Ru–Cl (bridging) distances are longer than the Ru–Cl (terminal) distances. These distances are comparable with the distances reported for other structurally characterized diruthenium(III) complexes containing bridging and terminal chlorides [56,57].

### 3.5. EPR spectra

EPR measurements of all the binuclear ruthenium complexes clearly demonstrate the presence of a rhombic ligand field component, as one might expect from the nature of the ligands around the metal ion. The EPR spectral profiles of the binuclear ruthenium(III) complexes (**1–6**) in frozen dichloromethane solutions are summarized in Table 5 and a representative spectrum is shown in Fig. 4. All the complexes show rhombic spectra with three distinct 'g' values ( $g_x \neq g_y \neq g_z$ ;  $g_x = 2.45$ – $2.55$ ;  $g_y = 2.04$ – $2.22$ ;  $g_z = 1.85$ – $1.96$ ) in decreasing order of magnitude. Such a rhombic distortion can be divided into axial (A) and rhombic (V) components. The axial distortion splits the t<sub>2</sub> level into 'a' and 'e' and the rhombic component again splits 'e' into non-degenerate components of the three major resonances, two are lower and one is higher than the field ~330 mT. The observed rhombicity of the spectrum is understandable in terms of the gross molecular symmetry of these complexes

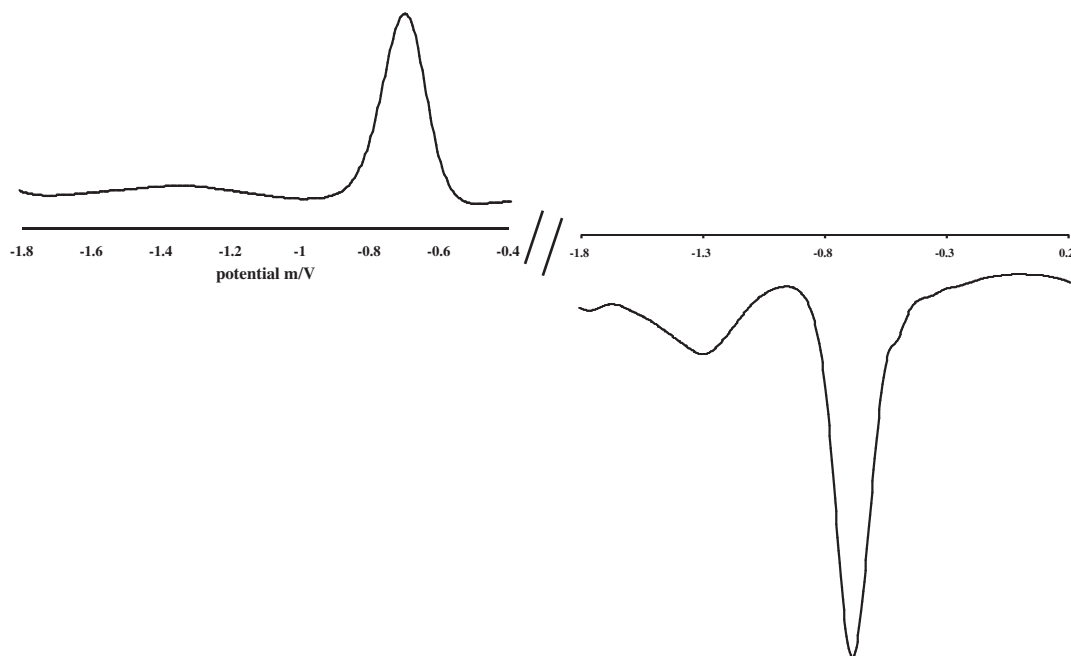
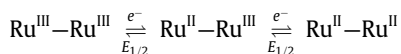


**Fig. 6.** Differential pulse voltammogram for the complex  $[\text{Ru}_2(\text{AsPh}_3)_2(\mu\text{-Cl})_2\text{Cl}_4(\text{L}_2)]$  (**5**) in 0.1 M  $\text{Bu}_4\text{NClO}_4$  in acetonitrile solution at 25 °C. The concentration of the complex =  $1 \times 10^{-3}$ ; the potential scan rate =  $2 \text{ mV s}^{-1}$ .

containing non-equivalent axes [58,47]. The presence of rhombic distortion is apparent in the splitting of the perpendicular resonance into two spaced components ( $g_x$  and  $g_y$ ). The EPR spectrum in Fig. 4 clearly contains a strong half-field resonance near 1300 G. That is a spin-forbidden transition, characteristic of dinuclear complexes with one unpaired electron on each ruthenium(III) atom ( $S = \frac{1}{2}$ ). Overall the position of the lines and the nature of the EPR spectra of the complexes are characteristics of low-spin ruthenium(III) octahedral complexes [56]. Hence, the results from the EPR spectral analysis indicate that these binuclear ruthenium(III) complexes are significantly distorted from the ideal octahedral geometry, as observed in the crystal structure of complex **2**.

### 3.6. Electron transfer properties

The electrochemical properties of all the binuclear ruthenium(III) complexes were studied in an oxygen free acetonitrile solution by cyclic voltammetry using a glassy carbon electrode and the potentials are expressed with reference to SCE. All the binuclear complexes ( $1 \times 10^{-3}$  M) are electroactive and exhibits two metal centered reductions in the potential range  $-0.62$  to  $-1.9$  V (0.05 M  $n\text{-Bu}_4\text{NClO}_4$  as the supporting electrolyte). The complexes display two successive Nernstian one electron quasi-reversible reductive responses ( $\text{Ru}^{\text{III}}\text{Ru}^{\text{III}} \rightleftharpoons \text{Ru}^{\text{III}}\text{Ru}^{\text{II}} \rightleftharpoons \text{Ru}^{\text{II}}\text{Ru}^{\text{II}}$ ) on the negative potential of the cyclic voltammogram at a scan rate of  $50 \text{ mVs}^{-1}$ . The potentials are summarized in Table 6 and a representative voltammogram (for **5**) is shown in Fig. 5. The redox processes are quasi-reversible in nature, characterized by a rather large peak to peak separation ( $\Delta E = 105\text{--}272$  mV). A comparison of the current heights ( $i_{\text{pa}}$ ) with that of the standard ferrocene/ferrocenium couple under identical experimental conditions reveals the processes to be one electron reductions [59,60].



The first reduction process takes place in the potential range  $E_{1/2} = -0.68$  to  $-0.74$  V ( $\Delta E = 105\text{--}137$  mV) and is attributed to the reduction of ruthenium(III) to the corresponding mixed-valence

complex. The second reduction response, observed at  $E_{1/2} = -1.25$  to  $-1.33$  V ( $\Delta E = 219\text{--}272$  mV), corresponds to the ruthenium(II) complex. A similar behavior has been recently observed for chloro bridged binuclear ruthenium(III) complexes [56].

Further, the differential pulse voltammograms of complex **5** reveals a feature associated with individual reduction steps on the negative side of the potential window, corresponding to the two pairs of peaks as observed in the cyclic voltammograms (Fig. 6).

## 4. Conclusion

The present work details the first investigation of new binuclear ruthenium(III) complexes bearing a pyridazine molecule. The bridging coordination nature of the pyridazine in these complexes was confirmed by a single crystal X-ray study and reveals the presence of a distorted octahedral geometry around ruthenium. Both ruthenium ions in the complexes are in the low spin state and display rhombic EPR spectra corresponding to the distorted octahedral geometry around the ruthenium(III) ion. All the complexes show two successive one electron quasi-reversible reductions ( $\text{Ru}^{\text{III}}\text{Ru}^{\text{III}}/\text{Ru}^{\text{III}}\text{Ru}^{\text{II}}$  and  $\text{Ru}^{\text{III}}\text{Ru}^{\text{II}}/\text{Ru}^{\text{II}}\text{Ru}^{\text{II}}$ ).

## Acknowledgments

Financial support by the Council of Scientific and Industrial Research (CSIR) New Delhi [Grant 01(2156)/07/EMR-II] is gratefully acknowledged. One of the authors, S.D.P., thanks CSIR for the award of Senior Research Fellowship (SRF). We thank DST-FIST, UGC-SAP India for X-ray, EPR and NMR facilities, School of Chemistry, Bharathidasan University, Tiruchirappalli.

## Appendix A. Supplementary data

CCDC 796684 contains the supplementary crystallographic data for complex **2**. These data can be obtained free of charge via <http://www.ccdc.cam.ac.uk/conts/retrieving.html>, or from the Cambridge

Crystallographic Data Centre, 12 Union Road, Cambridge CB2 1EZ, UK; fax: (+44) 1223-336-033; or e-mail: deposit@ccdc.cam.ac.uk.

## References

- [1] U. Beckmann, S. Brooker, *Coord. Chem. Rev.* 245 (2003) 17.
- [2] S. Brooker, R.J. Kelly, B. Moubaraki, K.S. Murray, *Chem. Commun.* (1996) 2579.
- [3] S. Brooker, P.G. Plieger, B. Moubaraki, K.S. Murray, *Angew. Chem., Int. Ed.* 38 (1999) 408.
- [4] S. Brooker, T.C. Davidson, S.J. Hay, R.J. Kelly, D.K. Kennepohl, P.G. Plieger, B. Moubaraki, K.S. Murray, E. Bill, E. Bothe, *Coord. Chem. Rev.* 216–217 (2001) 3.
- [5] Y. Lan, D.K. Kennepohl, B. Moubaraki, K.S. Murray, J.D. Cashion, G.B. Jameson, S. Brooker, *Chem. Eur. J.* 9 (2003) 3772.
- [6] P.G. Plieger, A.J. Downard, B. Moubaraki, K.S. Murray, S. Brooker, *Dalton Trans.* (2004) 2157.
- [7] I. Jess, C. Nather, *Inorg. Chem.* 42 (2003) 2968.
- [8] S. Brooker, J.D. Ewing, J. Nelson, J.C. Jeffery, *Inorg. Chim. Acta* 337 (2002) 463.
- [9] S. Brooker, J.D. Ewing, T.K. Ronson, C.J. Harding, J. Nelson, D.J. Speed, *Inorg. Chem.* 24 (2003) 2764.
- [10] T.K. Ronson, J. Nelson, G.B. Jameson, J.C. Jeffery, S. Brooker, *Eur. J. Inorg. Chem.* (2004) 2570.
- [11] L. Chen, L.K. Thompson, J.N. Bridson, *Can. J. Chem.* 70 (1992) 1886.
- [12] L. Chen, L.K. Thompson, S.S. Tandon, J.N. Bridson, *Inorg. Chem.* 32 (1993) 4063.
- [13] S. Brooker, R.J. Kelly, P.G. Plieger, *Chem. Commun.* (1998) 1079.
- [14] S. Brooker, S.J. Hay, P.G. Plieger, *Angew. Chem., Int. Ed.* 39 (2000) 1968.
- [15] L.K. Thompson, F.L. Lee, E.J. Gabe, *Inorg. Chem.* 27 (1988) 39.
- [16] L.K. Thompson, S.K. Mandal, J.P. Charland, E.J. Gabe, *Can. J. Chem.* 66 (1988) 348.
- [17] S.K. Mandal, L.K. Thompson, E.J. Gabe, J.P. Charland, F.L. Lee, *Inorg. Chem.* 27 (1988) 855.
- [18] D.R. Lide, *CRC Handbook of Chemistry and Physics*, 88th ed., Taylor & Francis, Boca Raton, 2007.
- [19] F. Abraham, M. Lagrenee, S. Sueur, B. Mernari, C. Bremard, *J. Chem. Soc., Dalton Trans.* (1991) 1443.
- [20] S.S. Tandon, L.K. Thompson, R.C. Hynes, *Inorg. Chem.* 31 (1992) 2210.
- [21] L. Chen, L.K. Thompson, J.N. Bridson, *Inorg. Chem.* 32 (1993) 2938.
- [22] L.K. Thompson, S.S. Tandon, M.E. Manuel, *Inorg. Chem.* 34 (1995) 2356.
- [23] J.C. Dewan, L.K. Thompson, *Can. J. Chem.* 60 (1982) 121.
- [24] M. Ghedini, G.D. Munno, G. Denti, A.M.M. Lanfredi, A. Tiripicchio, *Inorg. Chim. Acta* 57 (1982) 87.
- [25] S.K. Mandal, L.K. Thompson, A.W. Hanson, *J. Chem. Soc., Chem. Commun.* (1985) 1709.
- [26] L.K. Thompson, A.W. Hanson, B.S. Ramaswamy, *Inorg. Chem.* 23 (1984) 2459.
- [27] L.K. Thompson, *Can. J. Chem.* 61 (1983) 579.
- [28] L.K. Thompson, S.S. Tandon, *Comm. Inorg. Chem.* 18 (1996) 125.
- [29] K.V. Domasevitch, I.A. Gural'skiy, P.V. Solntsev, E.B. Rusanov, H. Krautscheid, J.A.K. Howard, A.N. Chernega, *Dalton Trans.* (2007) 3140.
- [30] M. Weitzer, S. Brooker, *Dalton Trans.* (2005) 2448.
- [31] J.E. Andrew, A.B. Blake, *J. Chem. Soc. A* (1969) 1408.
- [32] J.E. Andrew, P.W. Ball, A.B. Blake, *J. Chem. Soc., Chem. Commun.* (1969) 143.
- [33] P.W. Ball, A.B. Blake, *J. Chem. Soc. A* (1969) 1415.
- [34] P.W. Ball, A.B. Blake, *J. Chem. Soc., Dalton Trans.* (1974) 852.
- [35] G. Bullock, A. Cook, A. Foster, L. Rosenberg, L.K. Thompson, *Inorg. Chim. Acta* 103 (1985) 207.
- [36] L. Rosenberg, L.K. Thompson, E.J. Gabe, F.L. Lee, *J. Chem. Soc., Dalton Trans.* (1986) 625.
- [37] L.K. Thompson, S.K. Mandal, E.J. Gabe, J.P. Charland, *J. Chem. Soc., Chem. Commun.* (1986) 1537.
- [38] J.R. Price, N.G. White, A.P. Velasco, G.B. Jameson, C.A. Hunter, S. Brooker, *Inorg. Chem.* 47 (2008) 10729.
- [39] A. Escuer, R. Vicente, B. Mernari, A.E. Gueddi, M. Pierrot, *Inorg. Chem.* 36 (1997) 2511.
- [40] J.W. Slater, D.P. Lydon, N.W. Alcock, J.P. Rourke, *Organometallics* 20 (2001) 4418.
- [41] W.W. Sun, Q. Yue, A.L. Cheng, E.Q. Gao, *CrystEngComm* 10 (2008) 1384.
- [42] D. Donghi, G.D. Alfonso, M. Mauro, M. Panigati, P. Mercandelli, A. Sironi, P. Mussini, L.D. Alfonso, *Inorg. Chem.* 47 (2008) 4243.
- [43] K. Ohno, K. Arima, S. Tanaka, T. Yamagata, H. Tsurugi, K. Mashima, *Organometallics* 28 (2009) 3256.
- [44] K.R. Grünwald, G. Saischek, M. Volpe, F. Belaj, N.C.M. Zanetti, *Eur. J. Inorg. Chem.* (2010) 2297.
- [45] Y. Xu, A. Fischer, L. Duan, L. Tong, E. Gabriëlsson, B. Akermark, L. Sun, *Angew. Chem., Int. Ed.* 49 (2010) 8934.
- [46] G. Venkatachalam, R. Ramesh, S.M. Mobin, *J. Organomet. Chem.* 690 (2005) 3937.
- [47] S. Kannan, R. Ramesh, Y. Liu, *J. Organomet. Chem.* 692 (2007) 3380.
- [48] S. Kannan, M. Sivagamasundari, R. Ramesh, Y. Liu, *J. Organomet. Chem.* 693 (2008) 2251.
- [49] J. Chatt, G.J. Leigh, D.M.P. Mingos, R.J. Paske, *J. Chem. Soc. A* (1968) 2636.
- [50] K. Natarajan, R.K. Poddar, U. Agarwala, *J. Inorg. Nucl. Chem.* 39 (1977) 431.
- [51] G.M. Sheldrick, *SHELXS 97*, Program for the Solution of Crystal Structures, University of Gottingen, Germany, 1997.
- [52] G.M. Sheldrick, *SHELXL 97*, Program for the Refinement of Crystal Structures, University of Gottingen, Germany, 1997.
- [53] M. Nonoyama, K. Nakajima, K. Nonoyama, *Polyhedron* 20 (2001) 3019.
- [54] S. Kannan, R. Ramesh, *Polyhedron* 25 (2006) 3095.
- [55] S. Pal, S. Pal, *Inorg. Chem.* 40 (2001) 4807.
- [56] F.A. Cotton, M. Matusz, R.C. Torralba, *Inorg. Chem.* 28 (1989) 1516.
- [57] F.A. Cotton, R.C. Torralba, *Inorg. Chem.* 30 (1991) 2196.
- [58] O.K. Medhi, U. Agarwala, *Inorg. Chem.* 19 (1980) 1381.
- [59] G.K. Lahiri, S. Bhattacharya, M. Mukherjee, A.K. Mukherjee, A. Chakravorty, *Inorg. Chem.* 26 (1987) 3359.
- [60] P.K. Sinha, J. Chakravarty, S. Bhattacharya, *Polyhedron* 16 (1997) 81.